Current Shaping in a Hybrid 12-Pulse Rectifier Using a Vienna Rectifier

Ali Reza Izadinia and Hamid Reza Karshenas

***Abstract*—This paper presents a hybrid rectifier consisting of a 12-pulse rectifier in parallel with a Vienna rectifier. In the proposed structure, the 12-pulse rectifier supplies the bulk power to the load, whereas the Vienna rectifier shapes the input current to reduce its harmonic distortion. The unidirectional power flow of the Vienna rectifier results in undesirable distortion around the current zero crossing, which deteriorates current shaping in this region. To overcome this problem, besides current shaping, the Vienna rectifier is forced to participate in the active power. In this regard, the share of output power in each rectifier module must be calculated. To shape the input current, the reference current for the Vienna rectifier is generated using instantaneous power theory, and current tracking is carried out using the finite control set model predictive control. A detailed analysis of how to select the output power sharing ratio based on system losses and input current distortion is presented. The theoretical analysis is verified by using simulation and experimental results obtained from a 1 kW laboratory setup.**

***Index Terms*—12-pulse rectifier, current control, hybrid rectifier, model predictive control (MPC), Vienna rectifier.**

I. Introduction

HIGH-POWER rectifiers are widely used in industrial applications, such as the dc arc furnace, plasma arc torches, electrowinning, and traction substations. Rectifiers with the capability of supplying current as high as 350 kA have been reported [1]. The application of high-power rectifiers with semiconductor switches dates back to the 1960s when high-current diodes and thyristors were introduced [2]. For several years, diodes and thyristors have been the workhorses of high-power rectifiers in industry. These rectifiers, also known as line commutated rectifiers, are efficient, robust, reliable, and cost-effective and have been widely used for decades [3].

Line-commutated rectifiers suffer from a low power factor and harmonic-rich input current. Thus, their application in industry has recently been challenged due to the stringent requirements mandated by standards enacted for enhancing power quality in power systems. Much research has been conducted to reduce the harmonic distortion of the input current. Among various solutions, active rectifiers using forced commutated switches have received more attention than others [4]–[5]. Nevertheless, low efficiency, low reliability, and high cost have limited the applications of active rectifiers [6].

In an attempt to produce high-power rectifiers, "hybrid" rectifiers that benefit from the advantages of both passive (diode) and active rectifiers [6] have been proposed. Hybrid rectifiers employ parallel and/or series connections between a passive rectifier and an active rectifier [3], [6]. Regardless of the structure, any harmonic mitigation in a hybrid rectifier is usually carried out using the current control of the active part.

Current control of three-phase power electronic converters has always been an important and challenging topic. In past decades, the availability and development of powerful and fast microprocessors has evolved the way for implementing digital current control in power converters. One of the current control techniques with some interesting features is model predictive control (MPC) scheme. Predictive controllers use different approaches [7], but all use the model of converter and system to predict the future behavior of the controlled variable, e.g., the line current. Power converters are nonlinear systems in general, but consist of linear and nonlinear components and a finite number of switching devices. PID controllers for nonlinear, multiinput, multioutput (MIMO) systems with constraints are usually slow and cumbersome to design [8]. In the 1970s, MPC was developed to overcome the PID controller's problems.

Finite control set model predictive control (FCS-MPC) is a predictive control method used for active front–end rectifiers [9], [10], matrix converters [11], and multilevel inverters [7]. FCS-MPC minimizes a cost function defined based on the error between reference signal and control variable by selecting the optimum switching state of the system. This control scheme takes into account different constraints, such as minimizing the switching frequency [12], switching losses, or balancing the dc link voltage in a bipolar dc bus configuration [13]. In this control scheme, online optimization can be achieved, thanks to fast and powerful microprocessors. Furthermore, by eliminating the modulator in FCS-MPC, the control system complexity is reduced [7].

This paper proposes a hybrid rectifier consisting of a 12-pulse diode rectifier in parallel with a Vienna rectifier, as shown in Fig. 1. In this structure, the passive rectifier delivers the bulk power to the dc load, whereas the Vienna rectifier shapes the input current to mitigate harmonics injected by the 12-pulse rectifier. The proposed structure is a feasible solution for any new high-power rectifier, but can also find application in retrofit projects where a 12-pulse rectifier already exists but the

Manuscript received January 29, 2017; accepted March 6, 2017. Date of publication March 21, 2017; date of current version November 2, 2017. Recommended for publication by Associate Editor R. Redl.

The authors are with the Department of Electrical and Computer Engineering, Isfahan University of Technology, Isfahan 84156, Iran (e-mail: a.izadinia@ec.iut.ac.ir; karshen@cc.iut.ac.ir).

Color versions of one or more of the figures in this paper are available online at http://ieeexplore.ieee.org.

Digital Object Identifier 10.1109/TPEL.2017.2685459

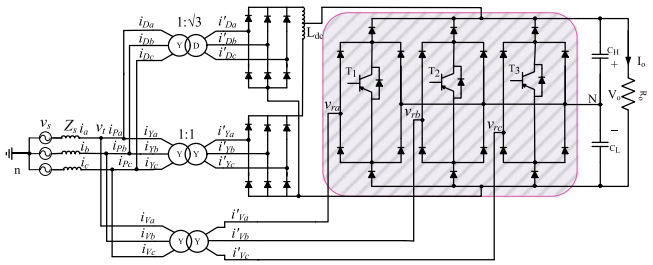

Fig. 1. Proposed hybrid rectifier—Vienna rectifier shown in dashed area.

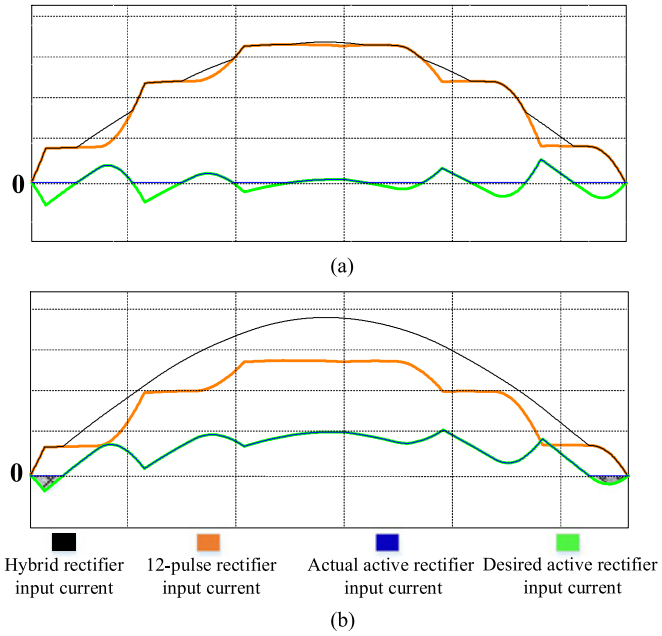

Fig. 2. Typical waveforms of the proposed hybrid rectifier with active filtering function of the Vienna rectifier. (a) Vienna rectifier does not participate in the active power. (b) Vienna rectifier takes a share of power.

harmonic distortion of the input current has to be reduced without bulky passive filters. The Vienna rectifier is a unidirectional converter and, thus, cannot perform active filtering around the current zero crossing which results in undesirable distortion. To overcome this limitation, the Vienna rectifier is forced to supply a portion of the active power. In this paper, the mathematical analysis of the optimum share of the Vienna rectifier in the proposed hybrid structure is presented. The instantaneous PQ theory [14] is used to extract the reference current for the Vienna rectifier, and the FCS-MPC is applied as a current control strategy.

The paper is organized as follows. In Section II, the proposed hybrid rectifier is introduced and its operating principle is explained. The procedure to implement instantaneous PQ theory and FCS-MPC is described in Section III. Sections IV and V validate the proposed control method using simulation and experimental results. The conclusions are presented in Section VI.

II. Proposed Hybrid Topology

In this section, the structure of the proposed hybrid rectifier along with its basic operation is presented. The mathematical expressions governing the operation of the proposed structure are derived. This analysis helps in finding the optimal operating point of the system based on the share of power that each subsystem takes.

A. Hybrid Rectifier Structure

Fig. 1 shows the structure of the proposed hybrid rectifier where a conventional 12-pulse rectifier is connected in parallel with a Vienna rectifier. The 12-pulse rectifier injects current harmonics with the order of $12k \pm 1$, where k is an integer. In many high-power applications, this level of harmonic distortion cannot be tolerated and does not meet power quality standards like the IEEE 519. Thus, the harmonic content of such a rectifier needs to be mitigated. In the proposed structure, while the 12-pulse rectifier provides the bulk power to the dc load, the Vienna rectifier performs three functions.

First, it provides an active filtering function for the input current of the 12-pulse rectifier. Second, it provides a bipolar dc output voltage for specific applications, such as high power electric vehicles (EV) charging stations [15]. Third, it contributes to a portion of load power so that better harmonic mitigation can be achieved. The latter function will be justified in the next paragraph. While other active-type rectifiers or active power filters can also be chosen in this structure, the Vienna rectifier is selected for this application as it has a mature structure with a reduced number of active switches which make it an attractive solution for such high-power applications [5]. A Vienna rectifier shown in Fig. 1 is a unidirectional converter in nature with no regeneration capability [16]. Therefore, it has limited capability for active filtering function. To show this limitation, consider Fig. 2, which illustrates the basic waveforms associated with the proposed structure for two operating points. Fig. 2(a) corresponds to the case when the Vienna rectifier provides active filtering function only. As can be seen, the improvement in input current distortion is minor due to the inability of the Vienna rectifier to inject negative current during the positive half cycle of voltage. Fig. 2(b) shows the case when the Vienna rectifier takes a share of output power. It can be seen that the input current has been significantly improved and only a small distortion is observed around current zero crossing.

It can be concluded from Fig. 2 that the amplitude of the fundamental current in the Vienna rectifier and consequently the amount of output power supplied by this rectifier has a direct influence on input current quality. In other words, the more the Vienna rectifier contributes to output power, the better quality of input current can be achieved. On the other hand, system cost and complexity increase as the active section, i.e., the Vienna rectifier, becomes larger. Therefore, it is more desirable to supply the majority of load power by the rugged 12-pulse rectifier, and hence, a tradeoff is necessary between the size of the Vienna rectifier and the quality of input current.

In the rest of this section, mathematical expressions governing the operation of the proposed structure are derived. Consequently, the optimum operating point of the proposed converter with respect to the share of power of each rectifier is calculated.

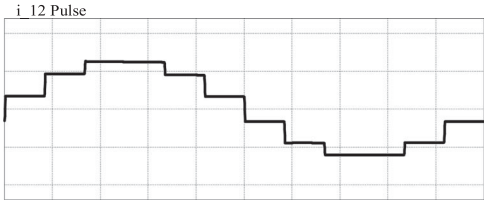

Fig. 3. Ideal 12-pulse rectifier input current.

B. Mathematical Analysis

The mathematical analysis of the proposed converter is performed with the following assumptions:

1) balanced three-phase operation with sinusoidal source voltage;
2) constant dc voltage;
3) ideal (loss-free) operation;
4) ignored high-frequency harmonics.

The notations used in the following analysis is based on what is shown in Fig. 1. Let us assume in this stage that the input current is also purely sinusoidal. Consequently, the instantaneous input power in the proposed rectifier is given by

$$p_{in} = v_{sa}\, i_a + v_{sb} i_b + v_{sc} i_c \tag{1}$$

where v_{sx} and i_x ($x = a, b, c$) are the instantaneous values of source phase voltage and current, respectively. Assuming a unity power factor operation, the average input active power is obtained as

$$P_{in} = p_{in} \;=\; 3 * V_s * I_s \tag{2}$$

where V_s and I_s are the rms values of source phase voltage and current, respectively. The instantaneous rectifier input current can now be obtained as

$$\begin{cases} i_a = \frac{\sqrt{2}P_{in}}{3V_s} * \sin(\omega t) \\ i_b = \frac{\sqrt{2}P_{in}}{3V_s} * \sin(\omega t - 120) \\ i_c = \frac{\sqrt{2}P_{in}}{3V_s} * \sin(\omega t + 120)\,. \end{cases} \tag{3}$$

The input current is composed of 12-pulse rectifier current plus the Vienna rectifier current. Fig. 3 shows a typical ideal waveform of input current in a 12-pulse rectifier. The mathematical expression for this waveform has been given in the appendix based on the average active power and other circuit parameters. In order to have sinusoidal input current, the current required by the Vienna rectifier in the positive half cycle can be calculated by subtracting (a.5) from (3), i.e.,

$$i_{Va} = \begin{cases} \frac{\sqrt{2}P_{in}}{3V_s}\sin(\omega t) - \frac{\sqrt{2}\pi}{36}\frac{P_P}{V_s}, & 0 \le \omega t \le 30 \\ \frac{\sqrt{2}P_{in}}{3V_s}\sin(\omega t) - \frac{\sqrt{2}\pi}{36}\frac{P_P}{V_s} - \frac{\sqrt{2}\pi}{12\sqrt{3}}\frac{P_P}{V_s}, & 30 \le \omega t \le 60 \\ \frac{\sqrt{2}P_{in}}{3V_s}\sin(\omega t) - \frac{\sqrt{2}\pi}{18}\frac{P_P}{V_s} - \frac{\sqrt{2}\pi}{12\sqrt{3}}\frac{P_P}{V_s}, & 60 \le \omega t \le 120 \\ \frac{\sqrt{2}P_{in}}{3V_s}\sin(\omega t) - \frac{\sqrt{2}\pi}{36}\frac{P_P}{V_s} - \frac{\sqrt{2}\pi}{12\sqrt{3}}\frac{P_P}{V_s}, & 120 \le \omega t \le 150 \\ \frac{\sqrt{2}P_{in}}{3V_s}\sin(\omega t) - \frac{\sqrt{2}\pi}{36}\frac{P_P}{V_s}, & 150 \le \omega t \le 180 \end{cases} \tag{4}$$

where P_P is the 12-pulse rectifier active power.

Inspection of (4) shows that for any ratio of P_P/P_{in}, the Vienna rectifier input current becomes negative in the intervals of $0 \le \omega t \le 30$ and $150 \le \omega t \le 180$ as the term $\frac{\sqrt{2}P_{in}}{3V_s}\sin(\omega t)$ becomes small around $\omega t = 0$ and $\omega t = \pi$. As stated in the beginning of this section, the Vienna rectifier shown in Fig. 1 is inherently incapable of drawing negative current during the positive half cycle of voltage. As a result, the Vienna rectifier cannot draw the current given by (4) during the whole positive half cycle, and a small distortion in the input current is unavoidable as shown in Fig. 2.

On the other hand, during the interval of $30 \le \omega t \le 150$, there is a ratio of P_P/P_{in} by which the Vienna rectifier input current always stays positive, thus making it possible to perform its active filtering and current shaping function adequately. Based on (4), it can be shown that if P_P/P_{in} is kept below 89%, the Vienna rectifier input current can always stay positive during the interval of $60 \le \omega t \le 120$ in the positive half cycle of input current.

This means that the Vienna rectifier needs to take only 11% of the total output power without violating the unidirectional power flow limit in the interval of $60 \le \omega t \le 120$. It should be noted that if the share of the Vienna rectifier output power is increased beyond the given value, the amount of distortion around current zero crossing is also decreased.

In reality, the 12-pulse rectifier input current is affected by different parameters such as source inductance, and hence, the current waveform becomes smoother than the ideal case. Therefore, the distortion around current zero crossing becomes smaller than the ideal case and hence the contribution of the 12-pulse rectifier in processing the active power can be increased.

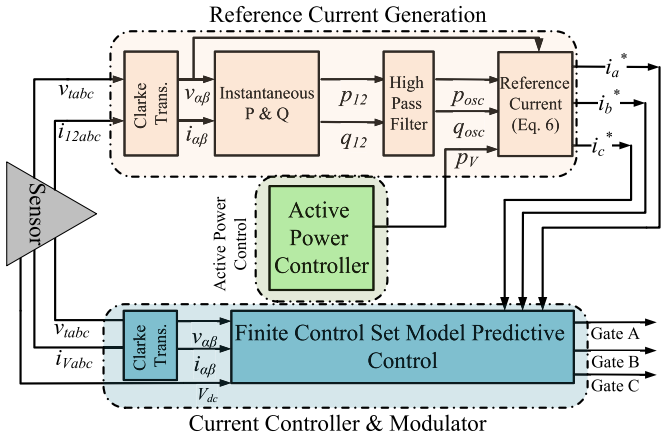

Fig. 4. Control System of the proposed hybrid rectifier.

III. Control System Implementation

The control system of the proposed hybrid converter is shown in Fig. 4. Three distinctive parts, shown in different colors, can be recognized from this control system as follows:

1) the Vienna rectifier reference current generation;
2) the Vienna rectifier active power controller;
3) finite control set MPC/modulator.

The main task of the proposed control system is to shape the Vienna rectifier input current to reduce harmonic distortion. Based on the discussion presented in Section II-B, while the

Vienna rectifier performs current shaping for harmonic mitigation, it also must participate in a portion of output power. Therefore, the first part of the proposed control system carries out reference current generation for current shaping, while the second part determines the share of active power of the Vienna rectifier. The third part of the controller takes care of proper reference tracking and modulation.

A. Vienna Rectifier Reference Current Generation

The main function of the Vienna rectifier in the proposed system is input current shaping for harmonic mitigation. Therefore, the harmonic content of the 12-pulse rectifier must be determined for proper compensation by the Vienna rectifier. In this regards, the instantaneous power theory [14] introduced in 1984 is employed to generate the required reference current for the Vienna rectifier. The procedure of generating reference current for the Vienna rectifier is depicted as a part of control system in Fig. 4. The first step is rewriting system variables in a two-phase (or $\alpha\beta$) stationary frame using the Clarke transformation. Consequently, the instantaneous active and reactive power, denoted by p and q, can be calculated. These powers can be decomposed into average ($\bar{p}$ and $\bar{q}$) and oscillating ($\tilde{p}$ and $\tilde{q}$) components as

$$\begin{bmatrix} p \\ q \end{bmatrix} = \begin{bmatrix} \bar{p} \\ \bar{q} \end{bmatrix} + \begin{bmatrix} \tilde{p} \\ \tilde{q} \end{bmatrix}. \tag{5}$$

Assuming sinusoidal voltage, the current distortion is due to the oscillatory component of power, i.e., $\tilde{p}$ and $\tilde{q}$. Therefore, by extracting the oscillatory component of instantaneous power, the reference currents in $\alpha\beta$-frame for the Vienna rectifier can be generated as

$$\begin{bmatrix} i_\alpha^* \\ i_\beta^* \end{bmatrix} = \frac{1}{{v_\alpha}^2 + {v_\beta}^2} \begin{bmatrix} v_\alpha & -v_\beta \\ v_\beta & v_\alpha \end{bmatrix} \begin{bmatrix} \tilde{p} \\ \tilde{q} \end{bmatrix} \tag{6}$$

where v_α and v_β are three-phase voltages in $\alpha\beta$ frame.

B. Vienna Rectifier Active Power Controller

As stated in Section II, the active power associated with the Vienna rectifier must be set to a value such that a distortion-free input current can be achieved. This preset value can be determined based on two control strategies described below.

1) Constant Power Strategy: In this strategy, the Vienna rectifier operates with its rated power irrespective of the total load power. As explained in Section II, to achieve low distortion input current, the Vienna rectifier must supply at least 11% of the total load. In the constant power strategy, the Vienna rectifier output power is set to 11% of the rated load and is kept fixed irrespective of output power. Therefore, when the load power demand is less than the rated value, the 12-pulse rectifier power decreases since the Vienna injected power is constant. In this strategy, an outer voltage loop assures proper output voltage control in case the total output power is less than the 11% of the rated value. An advantage of the constant power strategy is that the current distortion decreases as the load is lower than the rated value. On the other hand, the Vienna rectifier always operates at its full rating, resulting in higher losses associated with this rectifier.

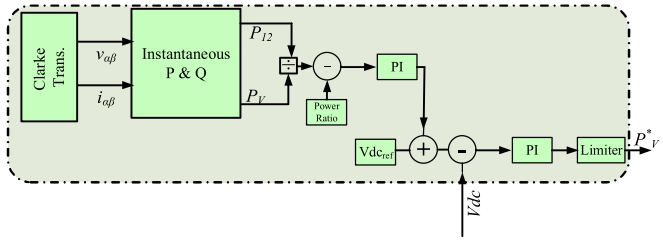

Fig. 5. Constant power ratio control strategy.

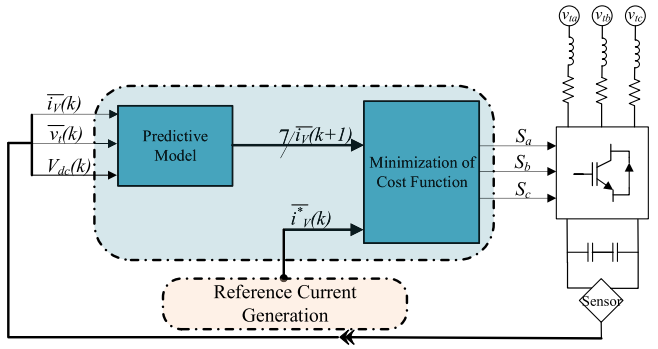

Fig. 6. Basic principle of predictive current control [18].

2) Constant Power Ratio Strategy: In this strategy, the ratio of power between the 12-pulse and the Vienna rectifier is kept fixed in all of operating conditions. Using this strategy calls for an additional control loop to determine the deviation of the dc link reference voltage in different operating points. The throughput active power of the uncontrolled 12-pulse rectifier can be controlled by controlling the dc link voltage. Therefore, the output power sharing ratio, defined as the ratio of the 12-pulse rectifier output power to total output power, can be controlled by output dc voltage control loop. Fig. 5 shows the block diagram for implementing this strategy.

C. Finite Control Set MPC/Modulator

As explained in the introduction, FCS-MPC is used where classic controllers are slow and the system is multiobjective and nonlinear. To implement this strategy, the following steps must be taken in the design stage [17]:

1) modeling the converter including all possible switching states;
2) defining the cost function based on the required performance;
3) discretizing the system model to predict the future state of the system and consequently selecting the optimum state which minimizes the cost function defined in 2.

The basic block diagram of the FCS-MPC used to implement the current control for the Vienna rectifier is shown in Fig. 6. In this control scheme, first the converter model (including input filter) is discretized. Consequently, the measured line currents $i_{Vx}(k)$ and input voltages $v_{tx}(k)$, where $x = a, b, c$, along with all switching states that can be selected in the next sampling

interval are applied to this model. Based on this information, a finite number of converter states (which is equal to the number of possible switching states) is predicted for the next sampling interval. Among these predicted states, the one which minimizes a cost function is selected and applied to the converter.

As explained above, the first step in implementing the FCS-MPC scheme is discretizing the rectifier model. To simplify the analysis, the transformer turns ratio is assumed to be 1. Writing KVL in Fig. 1 yields [9]

$$v_{tx} = L_V \frac{di_{Vx}}{dt} + R_V i_{Vx} + v_{rxN} - v_{nN}, x = a, b, c \quad (7)$$

where L_V and R_V are the input inductance and resistance of the Vienna rectifier and other parameters are defined in Fig. 1. Defining space-vector for three-phase quantities as $\bar{f} = \frac{2}{3}\ (f_a + af_b + a^2 f_c) = f_\alpha + jf_\beta$, where $\alpha = e^{j2\pi/3}$, and writing (7) in space-vector form yields

$$\bar{v}_t = L_V \frac{d}{dt}\left(\bar{i}_V\right) + R_V\left(\bar{i}_V\right) + \bar{v}_{rN} - \bar{v}_{nN} \quad (8)$$

where $\bar{v}_t$, $\bar{i}_V$, $\bar{v}_{rN,}$ and $\bar{v}_{nN}$ are the space vectors of different three-phase quantities. The last term in (8) is equal to zero since

$$(\bar{v}_{nN}) = \frac{2}{3} v_{nN}\ \left(1 + \alpha + \alpha^2\right) = 0. \quad (9)$$

Furthermore, $\bar{v}_{rN}$ in (8) can be expressed in terms of switching states and dc link voltage as

$$\bar{v}_{rN} = \bar{s}_r * V_{\rm dc} \quad (10)$$

where $\bar{s}_r$ is the switching state space-vector of the Vienna rectifier and $V_{\rm dc}$ is the dc link voltage. Substituting (9) and (10) in (8) and using the Euler forward method, (8) can be discretized as

$$\bar{i}_V\ (k+1) = \frac{T_s}{L_V}\ [\bar{v}_t\ (k) - \bar{s}_r * V_{dc}] + \left(1 - \frac{R_V L_V}{T_s}\right) \bar{i}_V\ (k) \quad (11)$$

where T_s is the sampling time. Equation (11) can be decomposed into real (α-axis) and imaginary (β-axis) parts as

$$\begin{aligned} i_{V\alpha}\ (k+1) &= \frac{T_s}{L_V}\left[v_{t\alpha}\ (k) - s_{r\alpha}\ (k) * \frac{V_{dc}}{2}\right] \\ &\quad + \left(1 - \frac{R_V L_V}{T_s}\right) i_{V\alpha}\ (k)) \\ i_{V\beta}\ (k+1) &= \frac{T_s}{L_V}\left[v_{t\beta}\ (k) - s_{r\beta}\ (k) * \frac{V_{dc}}{2}\right] \\ &\quad + \left(1 - \frac{R_V L_V}{T_s}\right) i_{V\beta}\ (k)). \end{aligned} \quad (12)$$

Now the cost function can be defined as

$$g = \left|i^*_{V\alpha} - i_{V\alpha}\right| + \left|i^*_{V\beta} - i_{V\beta}\right| \quad (13)$$

where $i^*_{V\alpha}$ and $i^*_{V\beta}$ are the real and imaginary parts of reference current vector ($\bar{i}^*_V = i^*_{V\alpha} + ji^*_{V\beta}$). Equation (14) is calculated for all possible switching states for the next sampling interval and eventually the switching state that minimizes (14) is selected.

TABLE I
SIMULATED AND EXPERIMENTAL SYSTEM PARAMETERS

Unit	Converter Parameters	Value
V_{rms}	Line to line ac voltage	385
Hz	Input line frequency	50
V	Reference dc link voltage	150
μF	dc side capacitors	1200
W	Converter rated power	1000
-	Vienna rectifier input transformer ratio	6:1
mH	Vienna rectifier input filter inductance	8
-	12-pulse rectifier *Y–Y* transformer ratio	3.5:1
mH	*Y–Y* Transformer leakage inductance	2
-	12-pulse rectifier Y-Δ transformer ratio	3.5:$\sqrt{3}$
mH	Y-Δ Transformer leakage inductance	2
Ω	Vienna rectifier input resistance	0.1
mH	dc link inductance	6
kHz	Sampling frequency	20

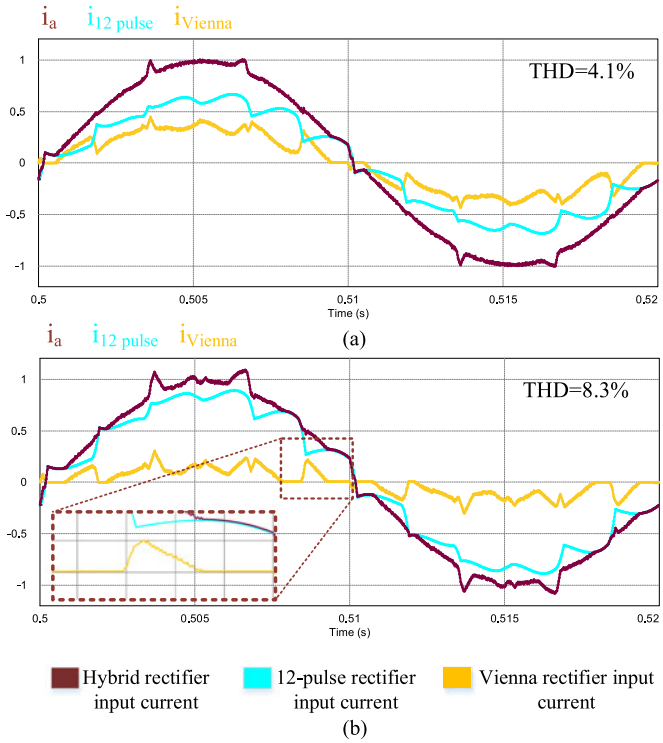

Fig. 7. Hybrid rectifier input current, 12-pulse rectifier input current, and Vienna rectifier input current—(a) output power sharing ratio is 65%, (b) output power sharing ratio is 90%.

IV. SIMULATION RESULTS

Using PSIM software, simulations were carried out to investigate the operation and performance of the proposed rectifier. Table I indicates the simulated system parameters. These parameters were chosen similar to the experimental system (explained in Section V) such that the agreement between simulation and experimental results can be better observed.

Fig. 7(a) shows the input current when the Vienna rectifier takes 35% of the output power, whereas Fig. 7(b) illustrates the same waveforms when the share of the Vienna rectifier has been reduced to 10%. As discussed in Section II, the higher the sharing of the Vienna rectifier, the better the quality of the

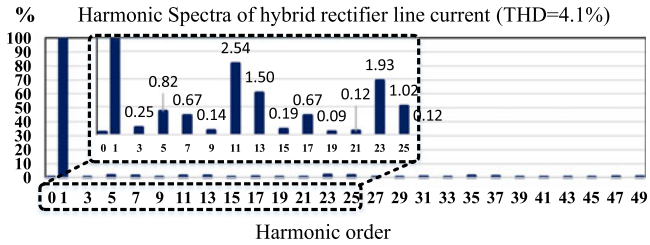

Fig. 8. Harmonic spectra of hybrid rectifier input current corresponding to Fig. 7(a).

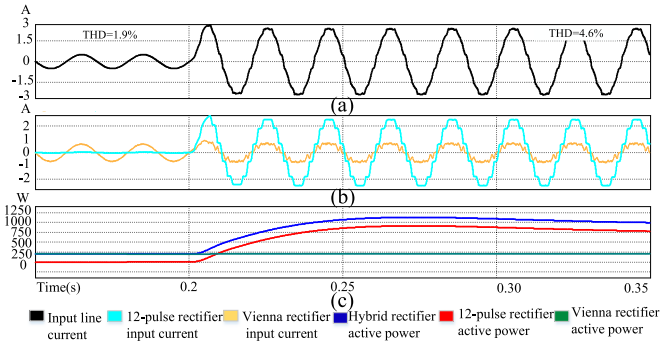

Fig. 9. Constant power control strategy with step load change applied at t = 0.205 s. (a) Input line current, (b) 12-pulse input current and Vienna rectifier input current, (c) active power of hybrid rectifier, 12-pulse rectifier and Vienna rectifier.

input current. This can also be realized by comparing the total harmonic distortion (THD) of input current in two cases. A close inspection of Fig. 7(b) (zoomed area) indicates how the Vienna rectifier has failed to wave-shape the 12-pulse rectifier current when its current tends to become negative in the positive half cycle of phase voltage. Fig. 8 shows the harmonic spectra of the input current corresponding to Fig. 7(a).

Fig. 9 illustrates input current and active power when the constant power strategy explained in Section III is employed. In this figure, a step load change from 25% to 100% has been applied to evaluate the output power sharing behavior of the system. As can be seen, the Vienna rectifier active power remains constant under all operating conditions, but the 12-pulse rectifier active power rises from nearly zero to its nominal value.

Fig. 10 shows similar waveforms as in Fig. 9 when the constant power ratio strategy explained in Section III is used. As can be seen, both the Vienna and 12-pulse rectifiers contribute in load active power, whereas the ratio of active power is kept constant. The THD shown in different operating conditions in these figures helps in understanding the performance of each strategy.

Fig. 11 represents the THD of the input current versus the output power sharing ratio (defined in Section III-B2). Furthermore, Fig. 12 shows the power loss associated with each rectifier module as the percentage of total output power versus output power sharing ratio. As expected, by increasing the output power sharing ratio, the THD of input current rises, but the total system losses decrease. These graphs can be used by a designer to select the optimum rating of each rectifier module based on different performance criteria such as the required input current distortion, the size of each rectifier module, and system efficiency.

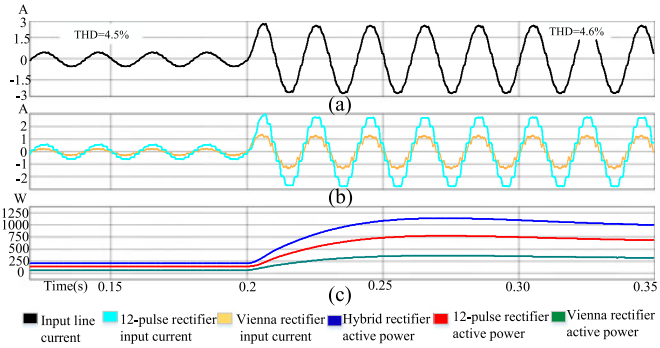

Fig. 10. Constant power ratio control strategy with step load change applied at t = 0.205 s. (a) Input current, (b) 12-pulse input current and Vienna rectifier input current, (c) active power of hybrid rectifier, 12-pulse rectifier and Vienna rectifier.

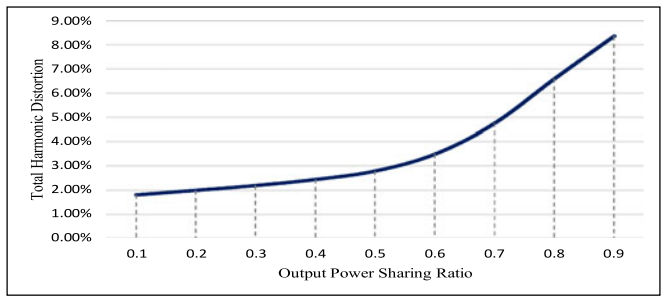

Fig. 11. THD of input current versus output power sharing ratio.

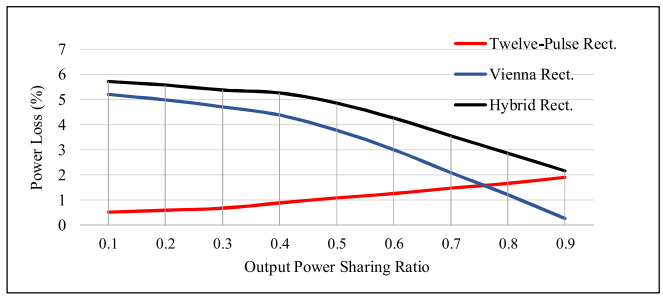

Fig. 12. Power loss of 12-pulse, the Vienna and hybrid rectifier versus output power sharing ratio.

V. Experimental Results

A 1 kW experimental setup was built to validate the theoretical analysis and results. The experimental setup parameters are listed in Table I. A DSP-based digital controller platform was used to implement the control system. Fig. 13 shows an overview of the experimental setup. Fig. 14 illustrates the input line current of the hybrid rectifier when the output power sharing ratio is 100% and the Vienna rectifier does not participate in the output power of the converter.

Fig. 15 shows different waveforms when the 12-pulse rectifier takes nearly 70% of total active power. In this figure, the

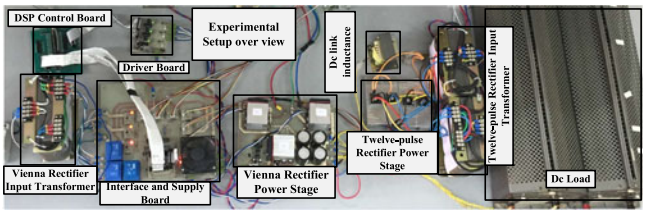

Fig. 13. Laboratory prototype of the proposed hybrid rectifier.

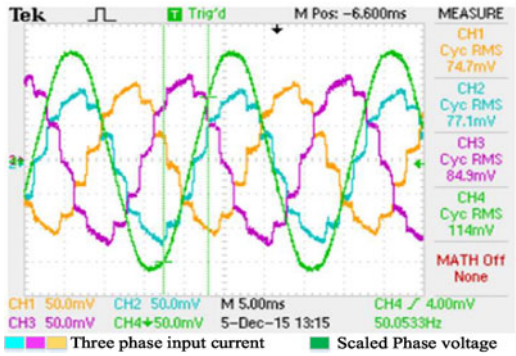

Fig. 14. Input line current of hybrid rectifier with scaled phase voltage when Vienna rectifier does not participate in output power.

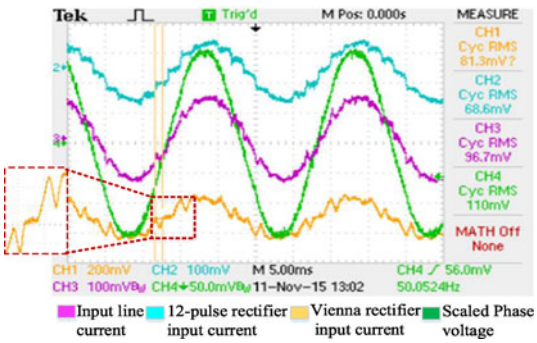

Fig. 15. 12-pulse rectifier input current, hybrid rectifier line current with scaled phase voltage, and Vienna rectifier input current.

current zero crossing region is also shown in the zoomed area when the Vienna rectifier has failed to wave-shape the 12-pulse rectifier current due to its unidirectional nature. In Fig. 16, the input current harmonic spectra with the THD equal to 4.7% are shown. Fig. 17 shows the system behavior when the output power sharing ratio is about 50%. As can be seen, line current distortion and notches are significantly reduced when the Vienna rectifier has more contribution in processing the output power in the hybrid converter. The line current THD corresponding to Fig. 17 is as low as 2.8%.

VI. Conclusion

This paper presented a hybrid rectifier consisting of a conventional 12-pulse rectifier in parallel with an active Vienna rectifier to achieve low-distortion input current. The parallel combination of two rectifiers allows the Vienna rectifier to act

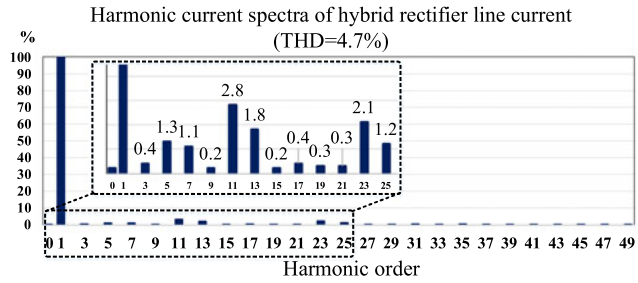

Fig. 16. Harmonic spectra of the proposed hybrid rectifier input current corresponding to Fig. 15.

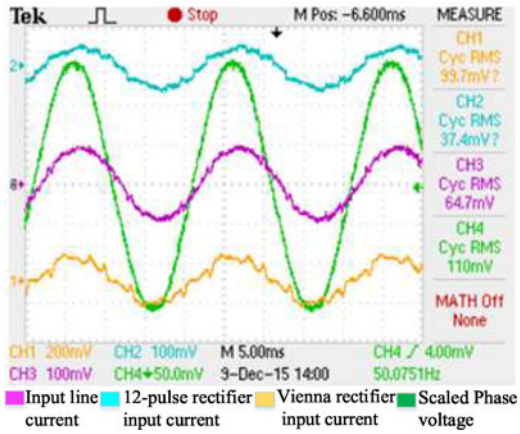

Fig. 17. Operation of hybrid rectifier when output power sharing ratio is about 50%.

as an active filter and compensate for 12-pulse rectifier input harmonics. However, the unidirectional nature of the Vienna rectifier leads to high current distortion around the current zero crossing. By allowing the Vienna rectifier to process a part of output power, this distortion can be significantly reduced. The mathematical expressions for obtaining the optimum operating point of each rectifier were obtained. A current controller based on FCS-MPC was used to manage the power sharing between two rectifiers. Simulation and experimental results on a 1 kW experimental setup were shown to validate the theoretical analysis. The proposed structure is a viable solution for any new high-power rectifier application. On the other hand, it can also find applications in retrofit projects where a 12-pulse rectifier already exists but its input current distortion is to be reduced to comply with new standards without adding bulky and sometimes troublesome passive filters.

Appendix

The notations used in this appendix are all referenced to Fig. 1. The ideal input current of a 12-pulse diode rectifier is depicted in Fig. 3. This current is composed of two 30° phased-shifted six-pulse diode rectifier input currents, i.e.,

$$i_{Px} = i_{Yx} + i_{Dx}, \qquad x = a, b, c \tag{a.1}$$

where i_P is the 12-pulse rectifier input current and i_Y and i_D are the input currents of *Y–Y* and *Y–D* transformers, respectively.

To simplify the following analysis, the turn ratio of the *Y–Y* transformer is assumed to be 1:1. The *Y–D* transformer input currents in phase *a* can be written as

$$i_{Da} = \frac{\sqrt{3}}{3}\left(i'_{Da} - i'_{Db}\right) \tag{a.2}$$

where i'_{Da} and i'_{Db} are the *Y–D* transformer output currents. Consequently, (a.1) in phase *a* can be rewritten as

$$i_{Pa} = i_{Ya} + \frac{\sqrt{3}}{3}\left(i'_{Da} - i'_{Db}\right). \tag{a.3}$$

By analyzing these waveform, the average dc current can be obtained as [6]

$$\bar{I}_{\mathrm{Ldc}} = \frac{P_D * \pi}{3\sqrt{6}V_s} \tag{a.4}$$

where P_D is the six-pulse rectifier active power with *Y–D* input transformer. Assuming the active power is equally shared between the *Y–Y* and *Y–D* transformers, and after some mathematical manipulations, the 12-pulse rectifier input current in phase a can be expressed by

$$i_{Pa} = \begin{cases} \frac{\sqrt{2}\pi}{36}\frac{P_P}{V_s}, & 0 \le \omega t \le 30 \\ \frac{\sqrt{2}\pi}{36}\frac{P_P}{V_s} + \frac{\sqrt{2}\pi}{12\sqrt{3}}\frac{P_P}{V_s}, & 30 \le \omega t \le 60 \\ \frac{\sqrt{2}\pi}{18}\frac{P_P}{V_s} + \frac{\sqrt{2}\pi}{12\sqrt{3}}\frac{P_P}{V_s}, & 60 \le \omega t \le 120 \\ \frac{\sqrt{2}\pi}{36}\frac{P_P}{V_s} + \frac{\sqrt{2}\pi}{12\sqrt{3}}\frac{P_P}{V_s}, & 120 \le \omega t \le 150 \\ \frac{\sqrt{2}\pi}{36}\frac{P_P}{V_s}, & 150 \le \omega t \le 180 \end{cases} \tag{a.5}$$

where P_P is the 12-pulse rectifier active power.

REFRENCES

[1] Y. Suh and P. K. Steimer, "Application of IGCT in high-power rectifiers," *IEEE Trans. Ind. Appl.*, vol. 45, no. 5, pp. 1628–1636, Sep./Oct. 2009.

[2] R. L. Alves, C. I. Font, and I. Barbi, "A novel unidirectional hybrid three-phase rectifier system employing boost topology," in *Proc. 2005 IEEE 36th Power Electron. Spec. Conf.*, 2005, pp. 487–493.

[3] R. L. Alves and I. Barbi, "Analysis and implementation of a hybrid high-power-factor three-phase unidirectional rectifier," *IEEE Trans. Power Electron.*, vol. 24, no. 3, pp. 632–640, Mar. 2009.

[4] R. Ghosh and G. Narayanan, "Control of three-phase, four-wire PWM rectifier," *IEEE Trans. Power Electron.*, vol. 23, no. 1, pp. 96–106, Jan. 2008.

[5] H. Yoo, K. Jang-Hwan, and S. Seung-Ki, "Sensorless operation of a PWM rectifier for a distributed generation," *IEEE Trans. Power Electron.*, vol. 22, no. 3, pp. 1014–1018, May 2007.

[6] T. B. Soeiro and J. W. Kolar, "Analysis of high-efficiency three-phase two-and three-level unidirectional hybrid rectifiers," *IEEE Trans. Ind. Electron.*, vol. 60, no. 9, pp. 3589–3601, Sep. 2013.

[7] V. Yaramasu, B. Wu, M. Rivera, and J. Rodriguez, "Predictive current control and DC-link capacitor voltages balancing for four-leg NPC inverters," in *Proc. IEEE Int. Symp. Ind. Electron.*, 2013, pp. 1–6.

[8] P. Karamanakos, T. Geyer, N. Oikonomou, F. D. Kieferndorf, and S. ' Manias, "Direct model predictive control: A review of strategies that achieve long prediction intervals for power electronics," *IEEE Ind. Electron. Mag.*, vol. 8, no. 1, pp. 32–43, Mar. 2014.

[9] M. Parvez, S. Mekhilef, N. M. L. Tan, and H. Akagi, "An improved active-front-end rectifier using model predictive control," in *Proc. IEEE Appl. Power Electron. Conf. Expo.*, 2015, pp. 122–127.

[10] D. E. Quevedo, R. P. Aguilera, M. A. Perez, P. Cortes, and R. Lizana, "Model predictive control of an AFE rectifier with dynamic references," *IEEE Trans. Power Electron.*, vol. 27, no. 7, pp. 3128–3136, Jul. 2012.

[11] M. Rivera, J. Rodriguez, W. Bin, J. R. Espinoza, and C. A. Rojas, "Current control for an indirect matrix converter with filter resonance mitigation," *IEEE Trans. Ind. Electron.*, vol. 59, no. 1, pp. 71–79, Jan. 2012.

[12] J. Holtz and S. Stadtfeld, "A predictive controller for the stator current vector of ac machines fed from a switched voltage source," in *Proc. Rec. Int. Power Electron. Conf.,* Tokyo, Japan, 1983, pp. 1665–1675.

[13] F. Rojas-Lobos, R. Kennel, and R. Cardenas-Dobson, "Current control and capacitor balancing for 4-leg NPC converters using finite set model predictive control," in *Proc. 39th Annu. Conf. IEEE Ind. Electron. Soc.*, 2013, pp. 590–595.

[14] H. Akagi, Y. Kanazawa, and A. Nabae, "Generalized theory of the instantaneous reactive power in three-phase circuits," in *Proc. Int. Power Electron. Conf.*, 1983, pp. 1375–1386.

[15] S. Rivera, B. Wu, S. Kouro, V. Yaramasu, and J. Wang, "Electric vehicle charging station using a neutral point clamped converter with Bipolar DC bus," *IEEE Trans. Ind. Electron.*, vol. 62, no. 4, pp. 1999–2009, Apr. 2015.

[16] J. W. Kolar and F. C. Zach, "A novel three-phase utility interface minimizing line current harmonics of high-power telecommunications rectifier modules," *IEEE Trans. Ind. Electron.*, vol. 44, no. 4, pp. 456–467, Aug. 1997.

[17] J. Rodriguez and P. Cortes, "Model predictive control," in *Predictive Control of Power Converters and Electrical Drives*. Hoboken, NJ, USA: Wiley, 2012, pp. 31–39.

[18] J. Rodriguez, J. Pontt, C. Silva, P. Cortes, U. Amman, and S. Rees, "Predictive current control of a voltage source inverter," in *Proc. IEEE 35th Annu. Power Electron. Spec. Conf.*, 2004, vol. 3, pp. 2192–2196.

Ali Reza Izadinia was born in Isfahan, Iran, in 1990. He received the B.Sc. degree in electrical engineering and the M.Sc. degree in power electronic & machine drive, in 2014 and 2016, respectively, both from Isfahan University of Technology, Isfahan, Iran.

Since 2016, he has been with Behrad Consulting Engineers, Isfahan, Iran, where he is currently the Senior Director of power quality and power electronic studies. His research interests include power converter design, power quality improvements, and harmonic source tracking in power system.

Hamid Reza Karshenas (M'08) received the B.Sc. degree from Isfahan University of Technology, Isfahan, Iran, in 1987, the M.Sc. degree from Sharif University of Technology, Tehran, Iran, in 1990, and the Ph.D. degree from the University of Toronto, Toronto, ON, Canada, in 1997, all in electrical engineering.

Since 1997, he has been with the Department of Electrical and Computer Engineering, Isfahan University of Technology, Isfahan, Iran, where he is an Associate Professor. He also has been working with The Queen's Centre for Energy and Power Electronics Research (ePOWER) as a research associate from 2009 till 2013. His research interests include power converter topologies, control in power electronics and application of power electronics in power system.